Desalination and Water Treatment
www.deswater.com

doi: 10.1080/19443994.2013.815587

52 (2014) 6282–6294
October

Taylor & Francis
Taylor & Francis Group

Wastewater treatment by ultrafiltration system, considering the effects of operating conditions: experimental and modeling

Amin Reyhani[a], Mahmood Hemmati[b,*]

[a]*Young Researchers and Elites Club, North Tehran Branch, Islamic Azad University, Tehran, Iran*
Tel. +98-912-2435963; Email: aminreyhani@gmail.com
[b]*Polymer Science and Technology Division, Research Institute of Petroleum Industry (RIPI), Tehran, Iran*
Email: hemmatim@ripi.ir

Received 27 February 2013; Accepted 7 June 2013

ABSTRACT

This study focuses on the effects of operating conditions including cross-flow velocity, oil concentration, transmembrane pressure, temperature, and pH on the normalized flux, relative fouling and turbidity rejection of a polymeric membrane in ultrafiltration (UF) system of oily wastewater treatment. Although normalized flux rose with increasing CFV, TMP, temperature, and pH, it decreased versus oil concentration. Increasing CFV, temperature, and pH reduced the relative fouling, while a rise in oil concentration and TMP increased the relative fouling. Moreover, an increase in CFV, oil content and pH increased turbidity rejection and rising TMP and temperature decreased the rejection. In this study, the evolutionary polynomial regression (EPR) approach is adopted on three parametric studies; one is the normalized flux, second is the relative fouling, and the third is the turbidity rejection. These parameters were evaluated by EPR as a function of mentioned independent variables. By comparing the experimental data and predicted values, the maximum and minimum average errors were obtained as 8.29 and 0.0005%, respectively. The maximum and minimum values of coefficient of determination were 1 and 0.902, respectively. Therefore, EPR would be a potential candidate to describe membrane performance in UF systems.

Keywords: Evolutionary polynomial regression; Normalized flux; Relative fouling; Turbidity rejection; Wastewater treatment

1. Introduction

Oily wastewaters are critical subject of environmental issues with high contents of oil are being generated in the petroleum industry [1]. In recent years membrane separation methods like microfiltration (MF), ultrafiltration (UF) [2], nanofiltration (NF), and reverse osmosis (RO) are being used for wastewater treatment [3]. The main drawback of membranes is fouling of their pore spaces and surfaces during the filtration process. Investigation of the fouling is worthwhile because fouling causes substantial flux declines during operation, affects selectivity negatively, increases the operational cost and requires frequent

*Corresponding author.

This article was originally published with an error in the list of corresponding authors. This version has been corrected. Please see Corrigendum (DOI: 10.1080/19443994.2013.850892)

membrane replacement. Therefore, knowledge about effect of operation conditions on fouling of membrane is essential [4]. One of the most important concerns in wastewater purification by membrane filtration is the removal of solutes. Recently, modeling the fouling of membrane and rejection rate evaluation have been the subject and challenging issue of many studies. Many researchers have represented their models in the cases of analytical modeling and modeling with machine learning such as genetic programming (GP) [5–7] and evolutionary polynomial regression (EPR) [8–10].

In GP, there is no need to have knowledge about neither the physics of the problem nor the design of the model. Shokrkar et al. [5] studied the treatment of oily wastewaters with synthesized ceramic MF membranes and proposed a new approach for modeling of flux membrane using GP. The results obtained from the GP model demonstrated acceptable fitness to the experimental data with an average error of less than 5%. Hwang et al. [6] modeled and predicted membrane fouling rate in a pilot-scale drinking water production system using GP to discover the mathematical function for the pattern of the membrane fouling rate. The model has adopted the input parameters for operating conditions (flow rate and filtration time) and feed water quality (turbidity, pH, temperature). The proposed model successfully simulated the pattern of membrane resistance during the operational period. Okhovat et al. [7] developed robust models based on experimental data to predict the membrane rejection of arsenic, chromium, and cadmium ions in a NF pilot scale system using GP. The results of the proposed GP models showed excellent concurrence with the experimental results. The performance and precisions of proposed GP models were quite satisfactory.

In the EPR, there are hybrid–capabilities of conventional numerical regression and GP. Savic et al. [8] modeled the number of collapses and blockages in two sewer systems using EPR to find the set of formula. Two approaches were implemented, first, two types of recorded sewer failures (collapses and blockages) observed during a five-year-period; second, the pipe data (age, size, etc.). The value of coefficient of determination (COD) was close to one that showed best fitness between experimental data and models.

In this study, the capability of EPR was applied as a powerful tool in order to make set of formula with a variable number of polynomial coefficients and find out the dependency of normalized flux, relative fouling, and turbidity rejection on independent variables, i.e. cross flow velocity (CFV), oil concentration, transmembrane pressure (TMP), temperature, and pH.

2. EPR in brief

Numerical regression as a powerful data analyzing method is commonly used to estimate the best fitting model for a set of experimental data. However, the type of a function (exponential, logarithmic, linear, etc.) must be selected before the fitting procedure commences. On the other hand, GP is considered as a simple and strong. Artificial intelligence-based strategy is utilized for computer learning inspired by natural evolution to find the suitable mathematical model to fit a set of points. The computer generates and evolves a whole population of functional expressions. The automated induction of mathematical descriptions of data using GP is usually referred to as symbolic regression [9]. EPR a synergistic technique, is a recently developed data-hybrid regression method by Giustolisi and Savic. This method integrates the best characteristics of GP with that of numerical regression. EPR consists of the set of equations including Case 0, Case 1, Case 2, and Case 3 as mentioned in previous studies [10,11].

Model accuracy, or fitness to observed data, is evaluated using the COD as follows [12]:

$$\mathrm{COD} = 1 - \frac{\sum_N (y - y_{\exp})^2}{\sum_N (y_{\exp} - \mathrm{avg}(y_{\exp}))^2} \quad (1)$$

And N is the number of experiments, y is the value predicted by the generated polynomial model, and $\mathrm{avg}(y_{\exp})$ is the average value of the corresponding observations. Eq. (1) shows that COD is strictly connected of cost functions [12]. Fig. 1 depicts the flowchart of EPR paces. In the left side of flowchart the steps of procedure have been shown. The prime steps consist of input data as EPR settings and that of user defined. Successive steps are evaluation of formula using Least Squares method. Eventually, the genetic algorithm used for the evolutionary stage of EPR that is employed to select the set of independent variables (X_i) that must form the model structure [13].

3. Materials and methods

3.1. Experimental setup

Fig. 2 shows a schematic diagram of the experimental applied setup in this study. The feed was pumped to the module by using centrifuge pump. While the pressure on the membrane was adjusted by valve V3, feed flow was regulated using valves V1 and V2.

The feed stream was split into two substreams, the concentrate which contained nonpassing components was returned to the feed tank, and the permeate flow

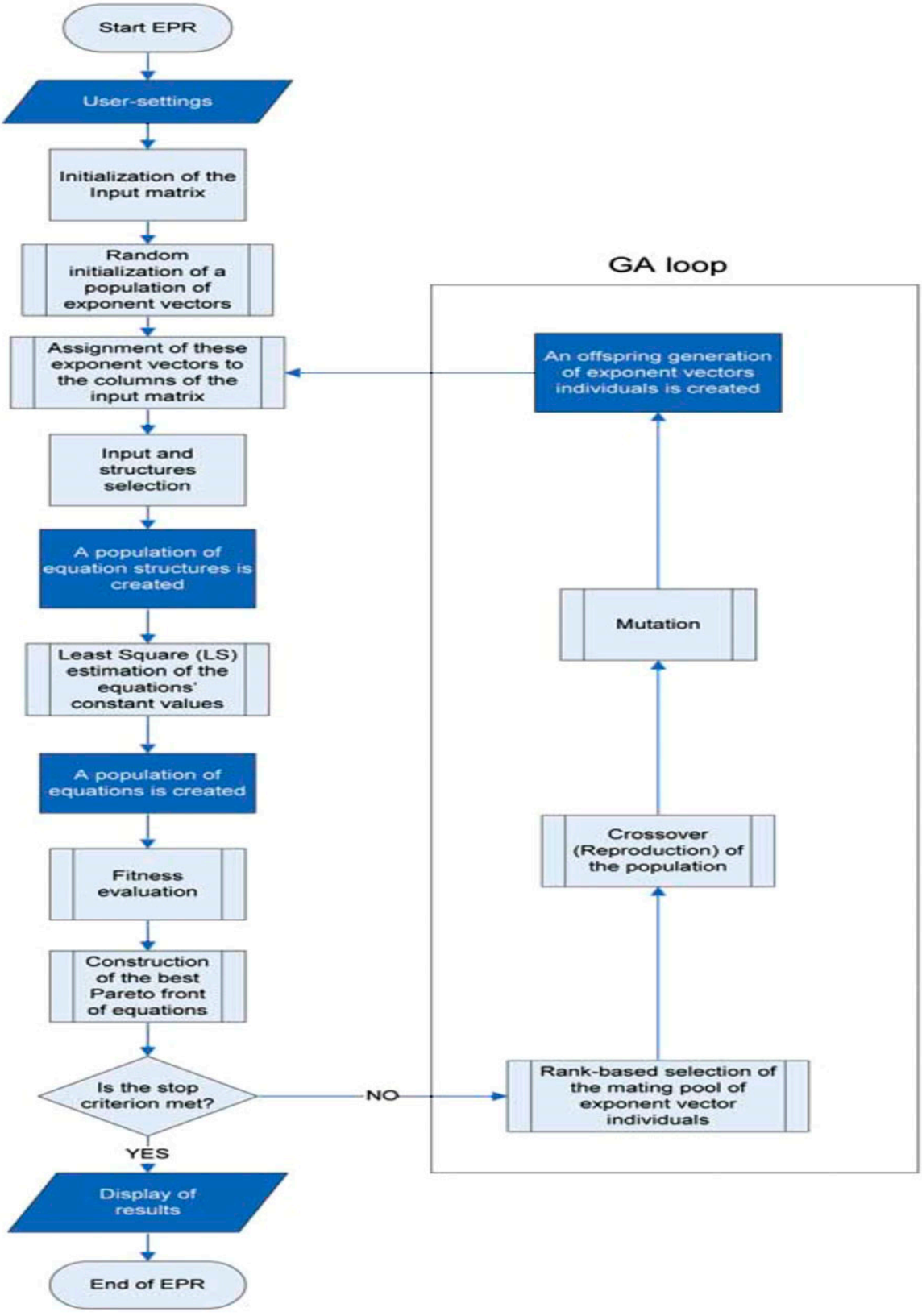

Fig. 1. The EPR flowchart [13].

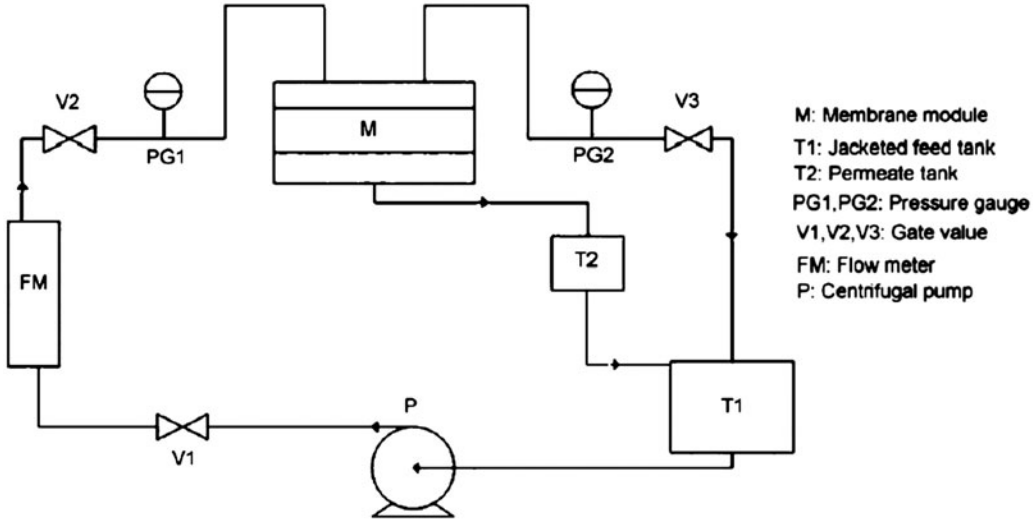

Fig. 2. Diagram of UF experimental set-up [14].

containing the components passed through the membrane and it was measured by a balance. The permeate flow, after measurement, was returned to the feed tank in order to have a constant concentration of the feed. As temperature is one of the controlling factors, a cooling/heating system was employed to detect the required temperature. All experiments were carried out in concentration mode of filtration for 150 min in a cross-flow operation.

3.2. Synthetic wastewater

The synthetic feed used in the experiments includes the following: gasoline, deionized water, and surfactant (Tween 85, Merck chemicals). This emulsion was made by gradual addition of gasoline to deionized water, mixed at 1,500 RPM using a finned mixer in 1.5 h. Before the addition of gasoline, the surfactant was dissolved in water for 10 min. Various emulsions with 0.1, 0.3, 0.6, 0.8, and 1 (%, v/v) of gasoline and a constant volume percent of surfactant (0.1 that of oil) were prepared. The size of particles with maximum percentage and the average size of particles in the synthetic feeds are reported in Table 1.

Table 1
Particles size with maximum percentage and average size of particles at different concentrations of emulsion

Oil concentration (%, v/v)	Size of particles in maximum percentage (nm)	Average size of particles (nm)
0.1	209	252
0.2	309	663
0.3	720	1,147
0.6	256–1936	1,271
0.8	1,535	1,551
1	2,531	3,898

3.3. Membrane characterization

A polymeric membrane formed from polyacrylonitrile (PAN), with a surface area of 66.15 cm^2, which was purchased from GE Osmonics Company, USA, was used in this study. Technical specifications of this membrane are given in Table 2.

The membrane fouling was observed with a scanning electron microscope (Philips XL30, Germany). The scanning electron microscope was operated with maximum voltage of 30 kV. Fig. 3 shows the SEM image of fresh YMMWSP1905 polymeric membrane. As it is clear before filtration, there is no cake layer on the membrane surface and no pore blocking on the pores. Some cracks on the SEM of the membrane surface are seen. It can be attributed to the additives used to increase in hydrophile characteristic of YMMWSP1905 membrane. In other word, when the company modified the membrane surface to improve hydrophile property of the YMMWSP1905 membrane,

Table 2
Characteristics of the polymeric membrane used in this study

Commercial name	YMMWSP1905
Material	Polyacrylonitrile (PAN)
MWCO[a] (kDa)	100
Typical Flux/bar (lit/m^2.hr.bar)	130
pH range (at 25°C)	2–9

[a]MWCO = Molecular weight Cut-off.

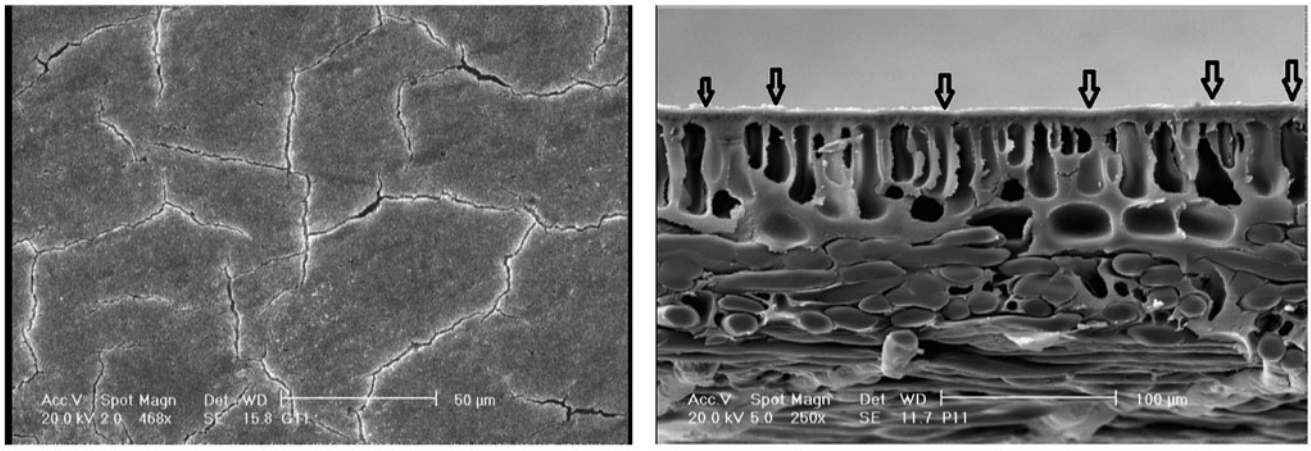

Fig. 3. SEM image of fresh YMMWSP1905 membrane, (a) Surface area, (b) Cross-section.

it made a great amount of unevenness on the surface. It is indicated in the cross-section micrograph in Fig. 3 (b) as well. Phenomenon such as this has also been reported in the previous researches [15–17].

4. Results and discussion

4.1. Experimental results

The values of normalized permeate flux, R_f/R_m or relative fouling and turbidity rejection obtained from experiments in the current UF system are concisely reported in Table 3 during variations of oil concentration and TMP.

4.2. EPR settings and models for relative fouling analysis using Matlab toolbox

The EPR settings used to provide the appropriate model are reported in Table 4. The type of regression was set static for the response parameters variations. The polynomial structure has been reported in Table 4. It was considered to enable EPR to select building blocks such as $f(X^{ES(j,K+1)} \ldots X^{ES(J,2K)}$ where X_i are input variables including; CFV(m/s), oil concentration (%, v/v), TMP (bar), temperature (°C), and pH.

As mentioned, in all experiments the values of normalized flux, relative fouling, and turbidity rejection depended on CFV, oil concentration, TMP,

Table 3
Experimental results during variations of oil concentration and TMP

CFV (m/s)	Oil concentration (%, v/v)	TMP (bar)	Temperature (°C)	pH (–)	Normalized permeate flux	R_f/R_m or relative fouling	Turbidity rejection (%)
1.5	**0.1**	3.5	30	7	2.04	0.04	94.94
1.5	**0.2**	3.5	30	7	1.87	0.08	96.22
1.5	**0.3**	3.5	30	7	1.76	0.11	97.06
1.5	**0.6**	3.5	30	7	1.74	0.19	98.78
1.5	**0.8**	3.5	30	7	1.72	0.26	98.82
1.5	**1**	3.5	30	7	1.70	0.33	98.94
1.5	0.3	**1**	30	7	0.80	0.11	99.94
1.5	0.3	**1.5**	30	7	1.20	0.12	99.68
1.5	0.3	**2**	30	7	1.47	0.12	99.53
1.5	0.3	**3**	30	7	1.72	0.15	99.29
1.5	0.3	**3.5**	30	7	1.80	0.16	99.32
1.5	0.3	**4**	30	7	2.08	0.17	99.12
1.5	0.3	**4.5**	30	7	2.15	0.19	99.06
1.5	0.3	**5.5**	30	7	2.32	0.23	98.85
1.5	0.3	**6**	30	7	2.44	0.26	98.79
1.5	0.3	**6.5**	30	7	2.50	0.28	98.50

Table 4
EPR settings

Regression type	Static
Polynomial structure	Case 0 of EPR equations [10]
Function of type	No function
Number of a_j	See figures
Range of exponents	[0, 0.5, 1, 2]
Offset (a_0)	Yes
Constant estimation method	Least squares
Number of generations	10

temperature, and pH. In each series of experiments, one of the variables varied while others were kept constant.

4.3. Influence of CFV

To investigate the effect of cross-flow velocity on the normalized flux, relative fouling, and rejection, the oil concentration, TMP, temperature, and pH were fixed at 0.30 (%, v/v), 3.5 bar, 30 °C and 7, respectively. Fig. 4(a) shows that with the rise of CFV, the normalized flux increased, in such a way that its value at velocity of 1.5 m/s is 40% higher than that at 1 m/s. Increasing CFV causes a rise in mass transfer coefficient in the concentration boundary layer and also increases the extent of mixing over the membrane surface [18]. Fig. 4(b) indicates the variation of relative fouling vs. CFV. Increasing CFV will intensify turbulence of fluid flow and severe shear forces will remove concentrated layer of precipitations from the membrane surface, which results in low fouling

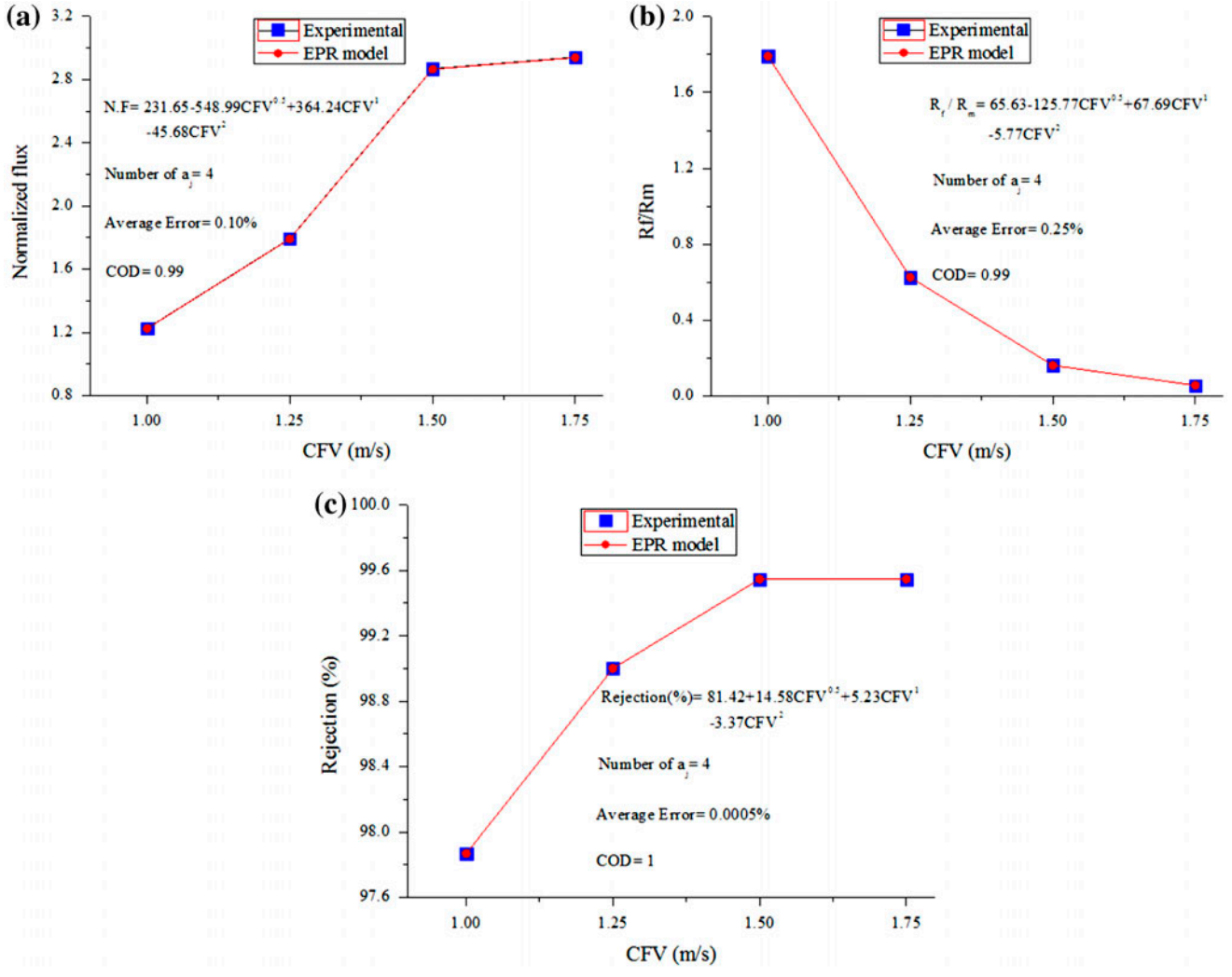

Fig. 4. (a) Normalized flux, (b) Relative fouling, (c) Rejection of turbidity, variations vs. CFV (Oil concentration = 0.30 (%, v/v), TMP = 3.5 bar, Temperature = 30 °C and pH = 7).

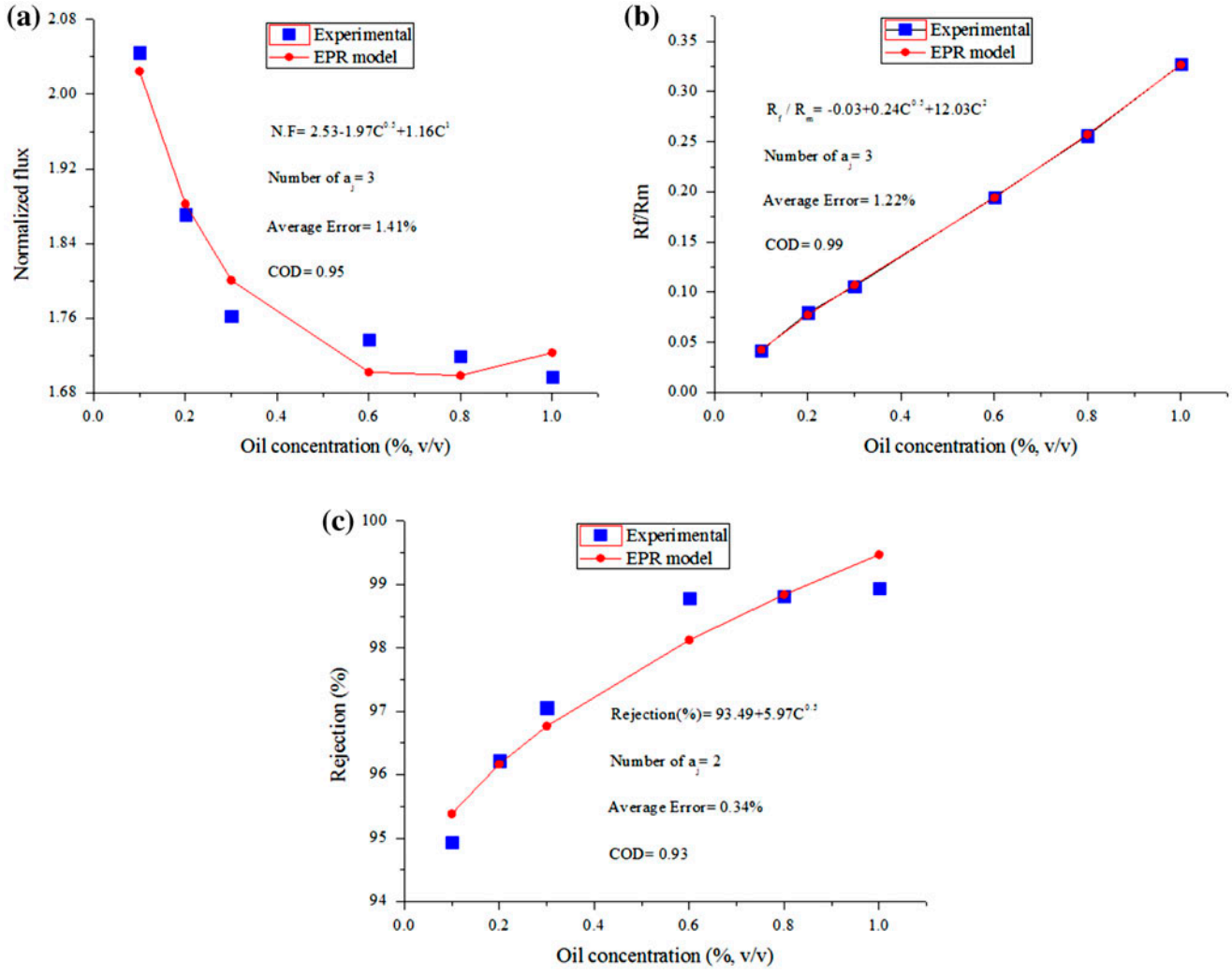

Fig. 5. (a) Normalized flux, (b) Relative fouling, (c) Rejection of turbidity, variations vs. oil concentration. (CFV = 1.5 m/s, TMP = 3.5 bar, Temperature = 30°C and pH = 7).

resistance. Therefore, at higher velocities, a part of created layer was detached from the membrane surface and returned to the liquid mass as a result of hydrodynamic effects of the flow [19]. Fig. 4(c) shows that the rejection rate rise with CFV which can be resulted from two probability: (1) Due to the remarkable hydrophilic character of YMMWSP1905 and also presence of severe turbulence in the stream, the retention time of particles on the surface of the membrane was reduced, therefore rejection increased. Under these circumstances, the reader may consider that in competition between water molecules and oil droplets, the water molecules dominated readily. (2) The rise of flow turbulence as a result of increasing the fluid velocity, led to the increase in number of efficient collisions between oil droplets. To prove these phenomena the particles size distribution of emulsion was measured at CFV = 1.5 m/s. It was observed that size of particles in maximum percentage increased dramatically from 720 nm to 3,500 nm. Here the values of average error were 0.10, 0.25, and 0.0005% (according to formula error (%) = $(Y_{exp} - Y)/Y_{exp} \times 100$), hereafter all error percentages are reported based on this equation), respectively, that shows a perfect fitness between experimental data and EPR prediction.

4.4. Influence of oil concentration

Fig. 5 shows a fine correspondence between experimental measurements and EPR model. In this stage the oil concentration was varied and the other parameters were kept constant. Table 1, proved that maximum size distribution of oil droplets increased with concentration. It means at high concentration, the average size of oil droplets at polarization layer was greater than that of the feed. Therefore, with increas-

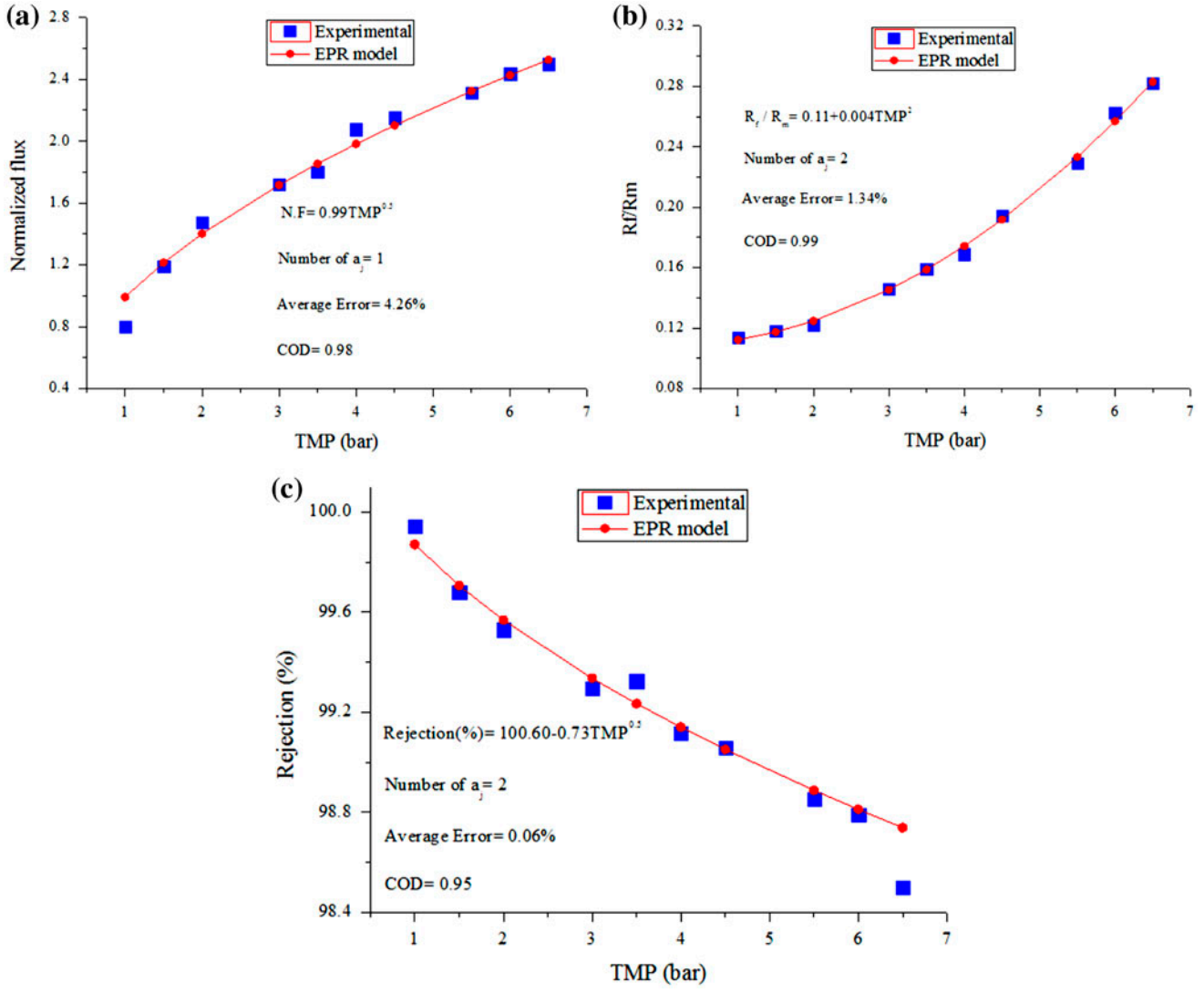

Fig. 6. (a) Normalized flux, (b) Relative fouling, (c) Rejection of turbidity, variations vs. TMP (CFV = 1.5 m/s, Oil concentration = 0.30 (%, v/v), Temperature = 30°C and pH = 7).

ing the oil contents on the feed side the thickness of the polarized layer on the membrane surface increased more readily. Thus, the oil droplets on the membrane surface pressed together and got more concentrated and finally reduced the normalized flux and increased the relative fouling of membrane. Previous studies also showed a similar behavior [14,20]. Fig. 5 (a) shows that normalized permeate flux always decreases with oil content. The average error for predicted values of normalized fluxes was 1.41%. Fig. 5 (b) illustrates relative fouling variations vs. oil concentration. Average error was 1.22%. According to Fig. 5(c), the rejection rate increased as a result of gel layer formation. The higher the oil concentration, the greater was the rejection rate. Okhovat et al. [7] modeled the behavior of rejection of arsenic, chromium, and cadmium by NF pilot-scale system using GP and obtained average errors 0.216, 0.836, and 1.796%, respectively. In this case, the average error value was 0.34%.

4.5. Influence of TMP

In this case, the values of CFV, oil concentration, temperature, and pH were fixed. Fig. 6 proves that EPR model has a good correspondence with the experimental values. According to Darcy's law, the pressure difference at two membrane sides brings about an increase in flux, although the effects of fouling limit increase [21,22]. Fig. 6(a) shows that normalized flux rose with increasing the TMP. The average error was 4.26%. Fig. 6(b) demonstrates the relative

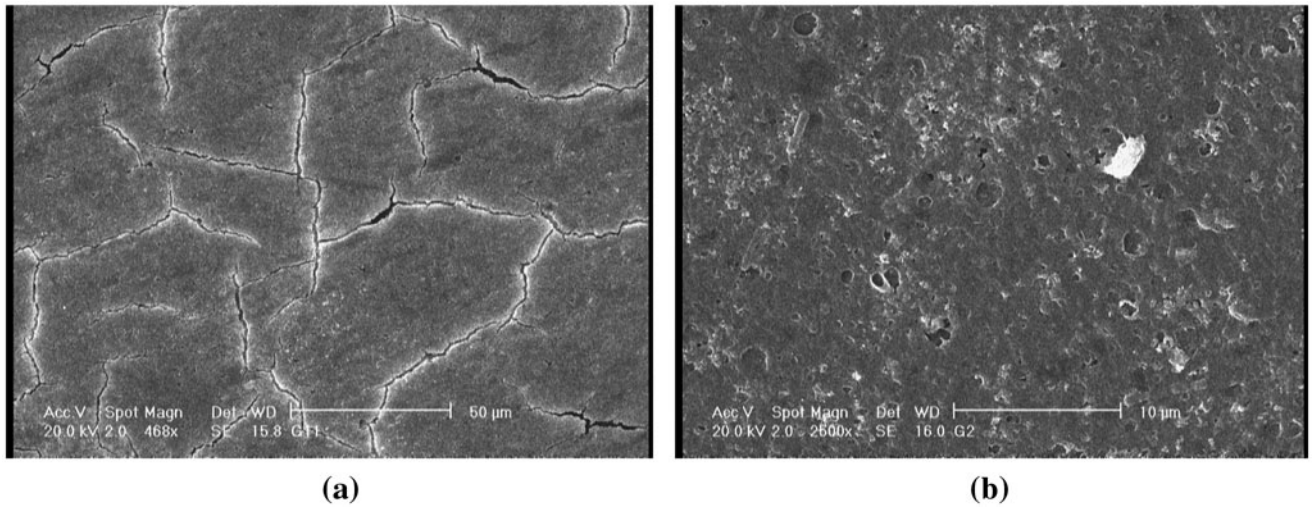

Fig. 7. SEM image of YMMWSP1905 membrane surface, (a) Before the filtration without gel layer, (b) At the end of the filtration with cake layer.

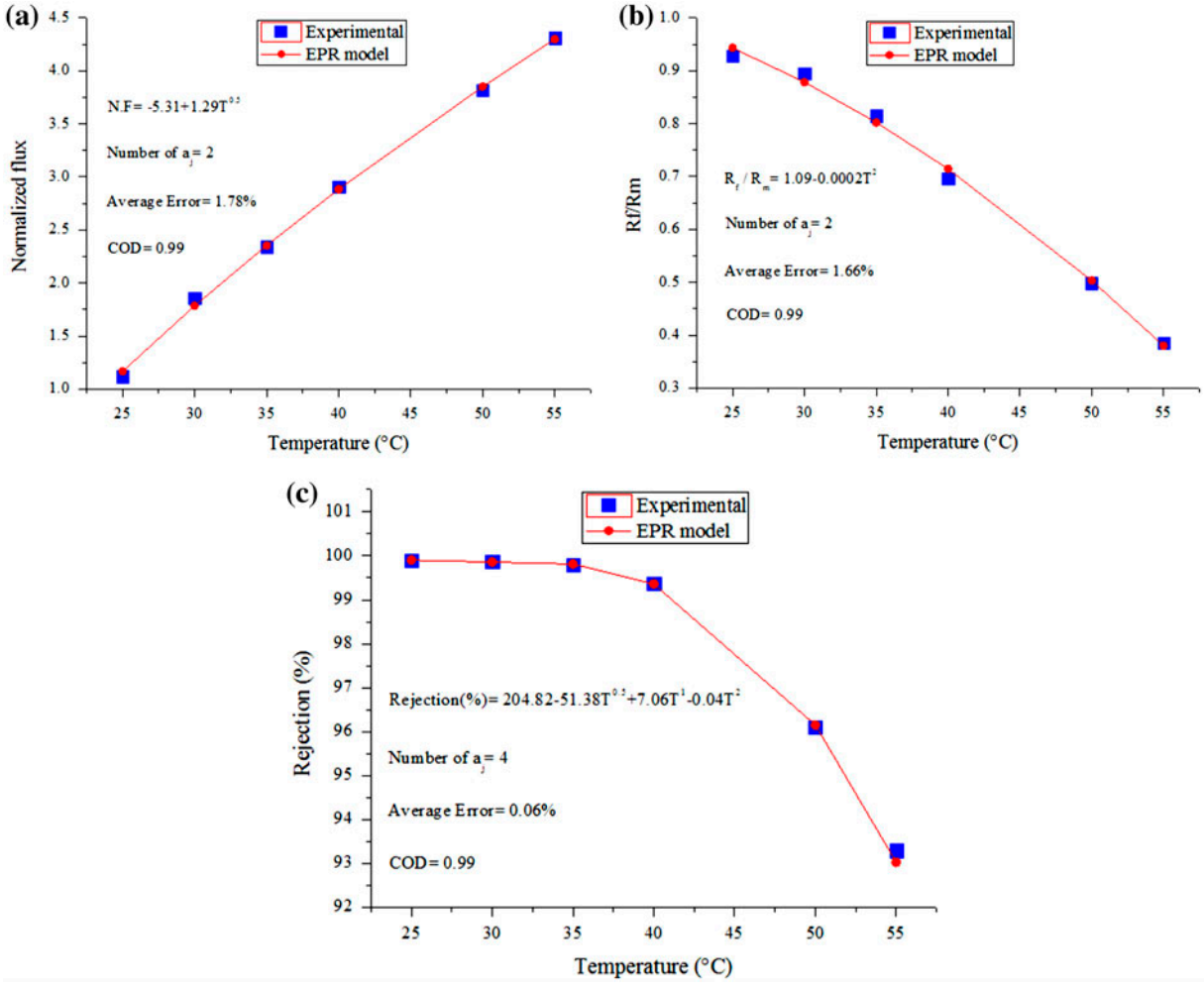

Fig. 8. (a) Normalized flux, (b) Relative fouling, (c) Rejection of turbidity, variations vs. temperature. (CFV = 1.5 m/s, Oil concentration = 0.30 (%, v/v), TMP = 3.5 bar and pH = 7).

fouling increased by TMP. By increasing in TMP, the concentration polarization phenomenon occurred on membrane surface; thus, the concentration difference between two membrane sides mounted [23]. Consequently, the diffusion driving force increased and more particles crossed the membrane and pore plugging that strongly resisted the permeation flow occurred by oil droplets [24]. This means that pore plugging is more likely to occur at higher levels of TMP. Rising of TMP makes the sediments compacted on the surface of membrane (Fig. 7(b)), and as a result, they block the membrane pores which cause more compression in internal fouling [21,22]. The value of average error for this part was 1.34%. Considering Fig. 6(c), the rejection decreased with pressure. This behavior can be attributed to the permeation of oil droplets through gel layer and membrane surface under the presence of high pressures. Average error value was 0.06% here.

Fig. 9(a) shows the surface of the membrane without any cake layer before UF and Fig. 9(b) indicates the existence of an oil layer on the membrane surface after UF process. The surface is covered by cake layer acting as a resistance in membrane filtration.

4.6. Influence of temperature

EPR model predicted a decrease in relative fouling and rejection rate, and an increase in normalized flux with increasing temperature. To investigate the effect of temperature, some experiments were done in the range of 25–55°C. The values of other independent variables were fixed at CFV = 1.5 m/s, oil concentration = 0.30 (%, v/v), TMP = 3.5 bar, and pH = 7, respectively. Previous researches have shown that an increase in temperature causes a rise in the amount of normalized permeate flux, as illustrated in Fig. 8(a) [25, 26]. The increase in temperature causes a reduction in the viscosity of solvent and, hence, an increase in the solvent diffusion coefficient [27, 28]. Average error was 1.78%. Likewise, increasing temperature caused a rise in the solubility of oil droplets in water, which caused that some droplets returned to feed flow and some of others penetrated onto the membrane (Fig. 9). These phenomena affected the thickness of gel layer in the way reduced it (Fig. 8(b)) [29]. Hwang et al. [6] reported 8% for average error using GP in polymeric membrane (PVDF) for prediction of membrane fouling in the pilot-scale MF system. The range of temperature in their study was set between 2.79°C and 22.58°C. In this case, the value of average error was 1.66%. Fig. 8(c) implies that the rejection of turbidity decreased with temperature due to two reasons: (1) increase of oil permeation, (2) reduction of fouling layer. By comparing experimental data and EPR prediction, the error average value was obtained as 0.06%. The values of average error prove that EPR model matches the experimental data as shown in Fig. 8.

4.7. Influence of pH

Fig. 10 compares the prediction quality of EPR model and the experimental measurements. The

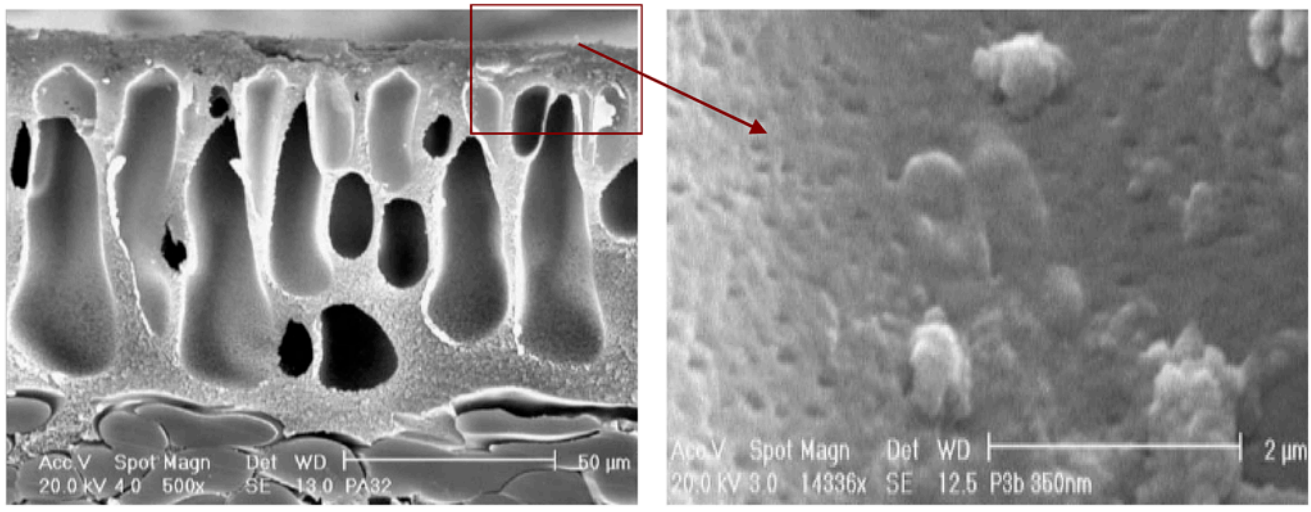

Fig. 9. SEM image of YMMWSP1905 membrane after UF process, (a) Cross section, (b) Sediments in the pores of membrane.

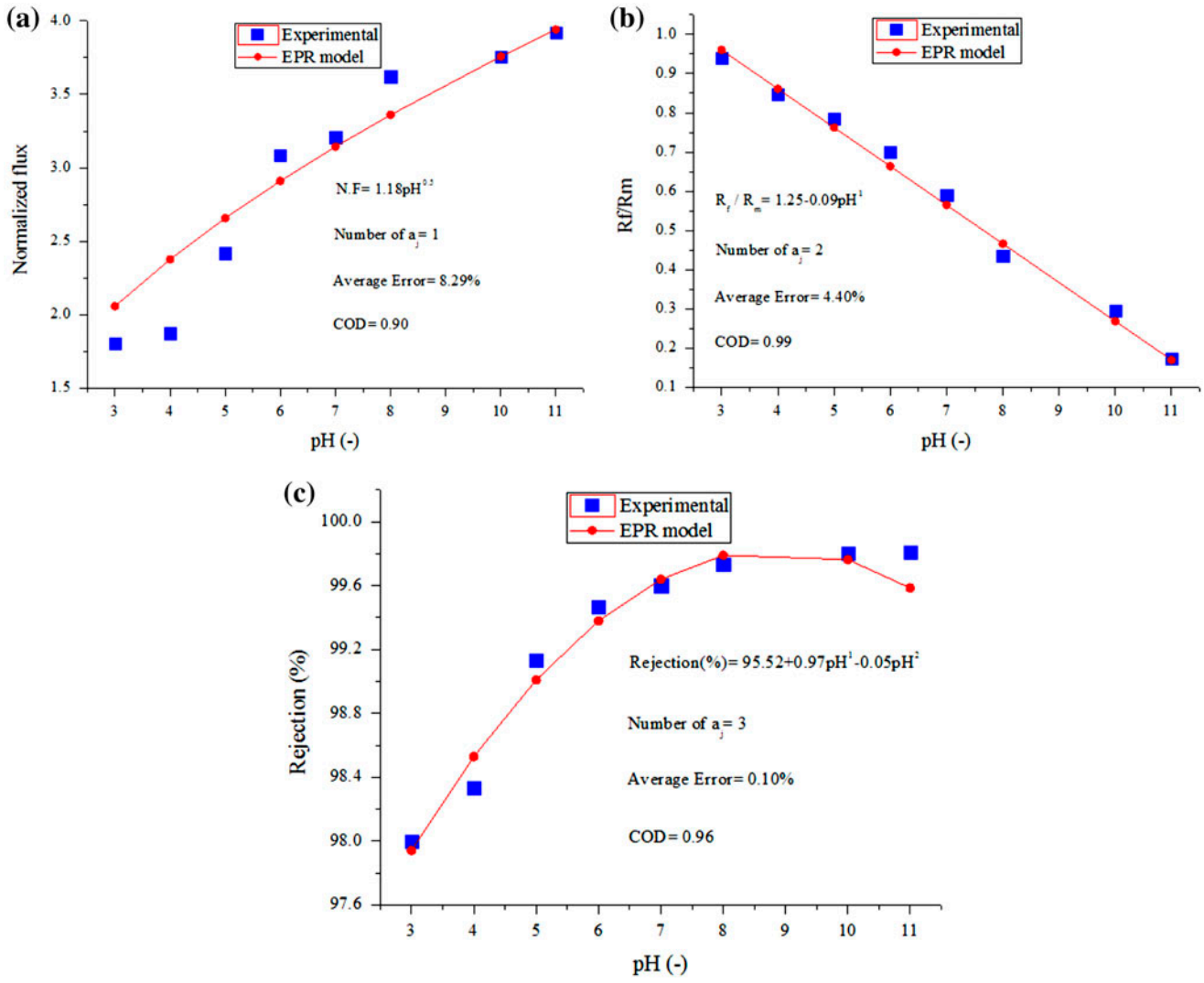

Fig. 10. (a) Normalized flux, (b) Relative fouling, (c) Rejection of turbidity, variations vs. pH. (CFV = 1.5 m/s, Oil concentration = 0.30 (%, v/v), TMP = 3.5 bar and Temperature = 30°C).

values of CFV, oil concentration, TMP, and temperature were chosen at 1.5 m/s, 0.30 (%, v/v), 3.5 bar, and 30°C, respectively. The rise in pH would increase the zeta potential value, so the thickness of cake that was generated by filtration would be reduced due to inter-droplet repulsion. Therefore, the feed solution would be more stable causing the normalized flux to increase and the relative fouling to decrease (Figs. 10 (a) and 10(b)). The values of average error for normalized flux and relative fouling predicted by EPR model were 8.29 and 4.40%, respectively. Furthermore, Fig. 10(c) shows that the rejection of turbidity increased by pH. In basic media, coagulation and aggregation of oil droplet occurs in which rejection percentage increases. Reader may attribute this phenomenon to the presence of supramolecular forces between oil droplets [30]. The value of average error was obtained as 0.10%.

4.8. Final results of EPR

To show the accuracy of EPR, some points in and out of the experimental ranges used in this study were selected. In these points the values of normalized flux, relative fouling, and turbidity rejection were measured during experiments, thereafter using EPR model the values of these parameters were predicted. As it is reported in Table 5, there is a good correspond between experimental data and the values predicted by EPR. By using the EPR models that

Table 5
Experimental and EPR results in order to prove the accuracy of EPR model

CFV (m/s)	Oil concentration (%, v/v)	TMP (bar)	Temperature (°C)	pH (–)	Experimental data			Predicted by EPR model		
					Normalized flux	R_f/R_m	Turbidity rejection (%)	Normalized flux	R_f/R_m	Turbidity rejection (%)
0.75	0.3	3.5	30	7	0.70	4.53	96.08	0.69	4.24	96.07
2	0.3	3.5	30	7	3.10	0.04	99.55	3.03	0.05	99.54
1.5	**0.4**	3.5	30	7	1.75	0.14	97.21	1.75	0.13	97.27
1.5	**0.7**	3.5	30	7	1.72	0.22	98.82	1.70	0.22	98.49
1.5	**0.9**	3.5	30	7	1.71	0.29	98.86	1.71	0.29	99.16
1.5	**1.2**	3.5	30	7	1.69	0.40	99.36	1.77	0.40	99.64
1.5	0.3	**0.5**	30	7	0.74	0.11	99.95	0.70	0.10	99.98
1.5	0.3	**2.5**	30	7	1.56	0.14	99.35	1.57	0.13	99.44
1.5	0.3	**5**	30	7	2.17	0.21	99.00	2.22	0.21	98.97
1.5	0.3	**7**	30	7	2.70	0.32	98.34	2.62	0.31	98.67
1.5	0.3	3.5	**45**	7	3.35	0.62	98.20	3.38	0.61	98.21
1.5	0.3	3.5	**60**	7	4.70	0.24	89.00	4.73	0.25	88.73
1.5	0.3	3.5	30	**2**	1.45	0.99	97.16	1.68	1.05	97.24
1.5	0.3	3.5	30	**9**	3.68	0.32	99.80	3.56	0.37	99.83
1.5	0.3	3.5	30	**12**	4.14	0.08	99.85	4.12	0.07	99.30

predict removal effeciency, the maximum level of turbidity rejection can be calculated. The maximum levels of turbidity removal occur when CFV = 2 m/s, oil concentration >1.2 (%, v/v), TMP < 0.5 bar, temperature <20 °C, and pH = 10. There is a difference in the pH part between maximum points obtained by EPR and the experiments; the experiments show pH = 12 as maximum point, while it is 10 achieved through EPR.

5. Conclusions

In this research, the influences of independent parameters, i.e. CFV, oil concentration, TMP, temperature, and pH on normalized flux, relative fouling, and turbidity rejection for a polymeric membrane in UF system were investigated. Increasing CFV, temperature, and pH, reduced the relative fouling, and increasing oil concentration and TMP caused an increase in the relative fouling. Also, it was shown that the increase in CFV, oil content, and pH would increase turbidity rejection and raising TMP and temperature would decrease the rejection.

EPR was used to predict the variations of normalized flux, relative fouling, and turbidity rejection. Predicted values for normalized flux and relative fouling were compared with measurements obtained by Darcy's law. Moreover, predicted values for the rejection of turbidity by EPR were compared with experimental values. This comparison demonstrated that EPR is suitable to be used in membrane UF process, because the maximum and minimum average errors were obtained as 8.29 and 0.0005%, respectively. Likewise, the maximum and minimum values of COD were 1 and 0.902, respectively.

Symbols

a_j — constant values in the formula obtained from EPR
avg (Y_{exp}) — the average value of the corresponding observations
COD — coefficient of determination
ES — matrix of exponents in the genetic algorithm
f — the function defined by the user in the EPR settings
X_i — vector of the k candidate inputs
Y — the value predicted by EPR
Y_{exp} — the value of observation in the experiment

References

[1] A. Asatekin, A.M. Mayes, Oil industry waste water treatment with fouling resistance membranes containing amphiphilic comb opolymers, Environ. Sci. Technol. 43 (2009) 4487–4492.
[2] J. Seo, A. Vogelpohl, Membrane choice for waste water treatment using external cross flow tubular membrane filtration, Desalination 249 (2009) 197–204.
[3] K. Nouzaki, J. Nagata, J. Arai, Y. Idemoto, N. Koura, H. Yanagishita, H. Negishi, D. Kitamoto, T. Ikegami, K. Haraya, Preparation of polyacrynitrile ultrafiktration membranes for waste water treatment, Desalination 144 (2002) 53–59.

[4] M. Pinelo, C. Ferrer, A.S. Meyer, G. Jonsson, Controlling the rejection of protein during membrane filtration by adding selected polyelectrolytes, Sep. Purif. Technol. 85 (2012) 54–60.
[5] H. Shokrkar, A. Salahi, N. Kasiri, T. Mohammadi, Prediction of permeation flux decline during MF of oily waste water using genetic programming, Chem. Eng. Res. Des. 90 (2012) 846–853.
[6] T.M. Hwang, H. Oh, Y.K. Choung, S. Oh, M. Jeon, J.H. Kim, S.H. Nam, S. Lee, Prediction of membrane fouling in the pilot-scale microfiltration system using genetic programming, Desalination 249 (2009) 285–294.
[7] A. Okhovat, S.M. Mousavi, Modeling of arsenic, chromium and cadmium removal by nanofiltration process using genetic programming, Appl. Soft Comput. 12 (2012) 793–799.
[8] D.A. Savic, O. Giustolisi, D.B. Laucelli, Asset performance analysis using multi-utility data and multi-objective data mining techniques, J. Hydroinform. 11 (2009) 211–224.
[9] V. Babovic, M. Keijzer, Genetic programming as a model induction engine, J. Hydroinform. 2 (2000) 35–61.
[10] O. Giustolisi, D. Laucelli, D.A. Savic, Development of rehabilitation plans for water mains replacement considering risk and cost-benefit assessment, Civil Eng. Environ. Syst. 23 (2006) 175–190.
[11] O. Giustolisi, A. Doglioni, D.A. Savic, B.W. Webb, A multi-model approach to analysis of environmental phenomena, Environ. Model. Softw. 22 (2007) 674–682.
[12] O. Giustolisi, L. Berardi, Water management challenges in global changes, London-GBR 1 (2007) 39–46.
[13] O. Giustolisi, A. Doglioni, D.A. Savic, F. di Pierro, An evolutionary multi-objective strategy for the effective management of groundwater resources, Water Resour. Res. 44 (2008) 1–14.
[14] A. Rezvanpour, R. Roostaazad, M. Hesampour, M. Nystrom, C. Ghotbi, Effective factors in the treatment of kerosene–water emulsion by using UF membranes, J. Hazard. Mater. 161 (2009) 1216–1224.
[15] L.S. Wan, Z.K. Xu, X.J. Huang, A.F. Che, Z.G. Wang, A novel process for the post-treatment of polyacrylonitrile-based membranes: Performance improvement and possible mechanism, J. Membr. Sci. 277 (2006) 157–164.
[16] Z.G. Wang, L.S. Wan, Z.K. Xu, Surface engineerings of polyacrylonitrile-based asymmetric membranes towards biomedical applications: An overview, J. Membr. Sci. 304 (2007) 8–23.
[17] G. Zhang, H. Meng, S. Ji, Hydrolysis differences of polyacrylonitrile support membrane and its influences on polyacrylonitrile-based membrane performance, Desalination 242 (2009) 313–324.
[18] A. Salahi, R. Badrnezhad, M. Abbasi, T. Mohammadi, F. Rekabdar, Oily wastewater treatment using a hybrid UF/RO system, Desalin. Water Treat. 28 (2011) 75–82.
[19] M. Hemmati, F. Rekabdar, A. Gheshlaghi, A. Salahi, T. Mohammadi, Effects of air sparging, cross flow velocity and pressure on permeation flux enhancement in industrial oily wastewater treatment using microfiltration, Desalin. Water Treat. 39 (2012) 33–40.
[20] M. Hlavacek, Break-up of oil-water emulsions induced by permeation through a microfiltration membrane, J. Membr. Sci. 102 (1995) 1–7.
[21] T. Mohammadi, A. Esmaeelifar, Wastewater treatment of a vegetable oil factory by a hybrid ultrafiltration-activated carbon process, J. Membr. Sci. 54 (2005) 129–137.
[22] M. Abbasi, M.R. Sebzari, A. Salahi, S. Abbasi, T. Mohammadi, Flux decline and membrane fouling in cross-flow microfiltration of oil-in-water emulsions, Desalin. Water Treat. 28 (2011) 1–7.
[23] S.S. Madaeni, A. Gheshlaghi, F. Rekabdar, Membrane treatment of oily wastewater from refinery processes, Asia-Pac. J. Chem. Eng. 8 (2012) 45–53.
[24] Z.B. Gonder, Y. Kaya, I. Vergili, H. Barlas, Optimization of filtration conditions for CIP wastewater treatment by nanofiltration process using Taguchi approach, Sep. Purif. Technol. 70 (2010) 265–273.
[25] P. Janknecht, D. Lopes, A.M. Mendes, Removal of industrial cutting oil from oil emulsions by polymeric ultra- and microfiltration membranes, Environ. Sci. Technol. 38 (2004) 4878–4883.
[26] M. Hesampour, A. Kryzaniak, M. Nystorm, Treatment of waste water from metal working by ultrafiltration, considering the effects of operating conditions, Desalination 222 (2008) 212–221.
[27] R.R. Sharma, R. Agrawal, S. Chellam, Temperature effect on sieving characteristics of thin-film composite nanofiltration membranes: Pore size distributions and transport parameters, J. Membr. Sci. 223 (2003) 69–87.
[28] I. Kowalska, K. Majewska-Nowak, M. Kabsch-Korbutowicz, Influence of temperature on anionic surface active agent removal from a water solution by ultrafiltration, Desalination 198 (2006) 124–131.
[29] S.S. Madaeni, The effect of large particles on microfiltration of small particles, J. Porous Mater. 18 (2001) 143–148.
[30] J.H.V. Esch, More than the sum of its parts, Nature 466 (2010) 193–194.